

Achromatic correction of diffractive dispersion in white light SLM imaging

Zdeněk Bouchal,^{1,*} Vladimír Chlup,¹ Radek Čelechovský,¹
Petr Bouchal,^{2,3} and Ioan Cristian Nistor¹

¹*Department of Optics, Palacký University, 17. listopadu 1192/12,
771 46 Olomouc, Czech Republic*

²*Institute of Physical Engineering, Faculty of Mechanical Engineering,
Brno University of Technology, Technická 2, 616 69 Brno, Czech Republic*

³*Central European Institute of Technology, Brno University of Technology,
Technická 10, 616 00 Brno, Czech Republic*

[*bouchal@optics.upol.cz](mailto:bouchal@optics.upol.cz)

Abstract: In contemporary optics, the spatial light modulator (SLM) is effectively used as a flexible optoelectronic device playing the key role in a number of experiments of science and technology. Its operation is optimal when using almost monochromatic light but an extremely strong diffractive dispersion occurs when white light is applied. In this paper, the design concepts are proposed resulting in optimization and implementation of a refractive corrector cooperating with the SLM. The corrector maintains the operation of the SLM unchanged for the central wavelength of light and ensures an achromatic dispersion compensation throughout the visible region in applications based on a lens-pattern formation. A significant improvement of the imaging performance of the achromatic SLM was proved by the computer simulation and measurement of the chromatic focal shift and the image contrast of the resolution target.

© 2014 Optical Society of America

OCIS codes: (230.6120) Spatial light modulators; (050.1965) Diffractive lenses; (260.2030) Dispersion; (110.3000) Image quality assessment.

References and links

1. B. J. Chang, L. J. Chou, Y. C. Chang, and S. Y. Chiang, "Isotropic image in structured illumination microscopy patterned with a spatial light modulator," *Opt. Express* **17**, 14710–14721 (2009).
2. C. Maurer, A. Jesacher, S. Bernet, and M. Ritsch-Marte, "What spatial light modulators can do for optical microscopy," *Laser Photon. Rev.* **5**, 81–101 (2011).
3. M. Reicherter, T. Haist, E. U. Wagemann, and H. J. Tiziani, "Optical particle trapping with computer-generated holograms written on a liquid-crystal display," *Opt. Lett.* **24**, 608–610 (1999).
4. J. Arines, V. Durán, Z. Jaroszewicz, J. Ares, E. Tajahuerce, P. Prado, J. Lancis, S. Bar, and V. Climent, "Measurement and compensation of optical aberrations using a single spatial light modulator," *Opt. Express* **23**, 15287–15292 (2007).
5. M. R. Beversluis, L. Novotny, and S. J. Stranick, "Programmable vector point-spread function engineering," *Opt. Express* **14**, 2650–2656 (2006).
6. Y. Esumi, M. D. Kabir, and F. Kannari, "Spatiotemporal vector pulse shaping of femtosecond laser pulses with a multi-pass two-dimensional spatial light modulator," *Opt. Express* **17**, 19153–19159 (2009).
7. M. D. Lew, S. F. Lee, M. Badirostami, and W. E. Moerner, "Corkscrew point spread function for far-field three-dimensional nanoscale localization of pointlike objects," *Opt. Lett.* **36**, 202–204 (2011).
8. T. Meeser, C. Falldorf, Ch. von Kopylow, and R. Bergmann, "Reference wave adaptation in digital lensless Fourier holography by means of a spatial light modulator," in *Optical Measurement Systems for Industrial Inspection*, Proc. of SPIE **8082**, 808206 (2011).

9. J. Rosen and G. Brooker, "Digital spatially incoherent Fresnel holography," *Opt. Lett.* **32**, 912–914 (2007).
10. S. Ngcobo, I. Litvin, L. Burger, and A. Forbes, "A digital laser for on-demand laser modes," *Nature Commun.* **4**, 2289 (2013).
11. S. Bernet, A. Jesacher, S. Furhaupt, Ch. Maurer, and M. Ritsch-Marte, "Quantitative imaging of complex samples by spiral phase contrast microscopy," *Opt. Express* **14**, 3792–3805 (2006).
12. R. Steiger, S. Bernet, and M. Ritsch-Marte, "SLM-based off-axis Fourier filtering in microscopy with white light illumination," *Opt. Express* **20**, 15377–15384 (2012).
13. M. S. Millán, J. Otón, and E. Pérez-Cabré, "Dynamic compensation of chromatic aberration in a programmable diffractive lens," *Opt. Express* **14**, 9103–9112 (2006).
14. P. Bouchal, J. Kapitán, Radim Chmelfk, and Z. Bouchal, "Point spread function and two-point resolution in Fresnel incoherent correlation holography," *Opt. Express* **19**, 15603–15620 (2011).
15. X. Lai, S. Zeng, X. Lv, J. Yuan, and L. Fu, "Violation of the Lagrange invariant in an optical imaging system," *Opt. Lett.* **38**, 1896–1898 (2013).
16. J. Rosen, N. Siegel, and G. Brooker, "Theoretical and experimental demonstration of resolution beyond the Rayleigh limit by FINCH fluorescence microscopic imaging," *Opt. Express* **19**, 26249–26268 (2011).
17. P. Bouchal and Z. Bouchal, "Selective edge enhancement in three-dimensional vortex imaging with incoherent light," *Opt. Lett.* **37**, 2949–2951 (2012).
18. P. Bouchal and Z. Bouchal, "Concept of coherence aperture and pathways toward white light high-resolution correlation imaging," *New J. Phys.* **15**, 123002 (2013).
19. R. Kingslake and R. B. Johnson, *Lens Design Fundamentals* (Elsevier, 2010).
20. T. Stone and N. George, "Hybrid diffractive-refractive lenses and achromats," *Appl. Opt.* **27**, 2960–2971 (1988).
21. J. Li, Ch. H. Wen, S. Gauza, R. Lu, and S. T. Wu, "Refractive indices of liquid crystals for display applications," *J. Display Technol.* **1**, 1551–1561 (2005).
22. A. Flores, M. R. Wang, and J. J. Yang, "Achromatic hybrid refractive-diffractive lens with extended depth of focus," *Appl. Opt.* **43**, 5618–5630 (2004).
23. N. Davidson, A. Friesem, and E. Hasman, "Analytic design of hybrid diffractive-refractive achromats," *Appl. Opt.* **32**, 4770–4774 (1993).
24. E. Tajahuerce, V. Climent, J. Lancis, M. Fernández-Alonso, and P. Andrés, "Achromatic Fourier transforming properties of a separated diffractive lens doublet: theory and experiment," *Appl. Opt.* **37**, 6164–6173 (1998).
25. V. Moreno, J. F. Román, and J. R. Salgueiro, "High efficiency diffractive lenses: Deduction of kinoform profile," *Am. J. Phys.* **65**, 556–562 (1997).
26. D. A. Buralli and G. M. Morris, "Effects of diffraction efficiency on the modulation transfer function of diffractive lenses," *Appl. Opt.* **31**, 4389–4396 (1992).
27. N. Davidson, R. Duer, A. A. Friesem, and E. Hasman, "Blazed holographic gratings for polychromatic and multidirectional incidence light," *J. Opt. Soc. Am. A* **9**, 1196–1199 (1992).

1. Introduction

The SLMs are devices using MEMS (Micro Electro Mechanical Systems) or LCD (Liquid Crystal Display) technology for a real-time amplitude or phase modulation of optical waves in space. The SLM can flexibly fulfill the role of conventional optical elements or replace the function of several elements at once. It may even provide operations inaccessible by other optical means. For the versatility and simplicity of integration, the SLMs were successfully deployed in diverse areas of optics and enabled a variety of important applications including structured illumination [1] and novel imaging techniques in microscopy [2], holographic optical tweezing [3], adaptive correction of aberrations [4], point spread function (PSF) engineering [5], spatio-temporal vector shaping of laser pulses [6], particle localization and tracking by a spiral modulation in optical systems with the rotating PSF [7], adaptation of reference wave in interferometry and digital holography [8] or light splitting and shaping in Fresnel incoherent correlation holography (FINCH) [9]. Quite recently, the SLM was used as an intra-cavity holographic mirror enabling on-demand generation of laser modes in the digital laser [10].

The LCOS (Liquid Crystal On Semiconductor) SLM discussed in this paper uses optical and electrical anisotropy of liquid crystal (LC) materials to modulate transmitted or reflected light waves. The optical properties of the device depend on the alignment layers of the LC cells. The most important cases include parallel or vertical aligned cells or twisted cells. Depending on the polarization configuration, amplitude or phase modulation of light may be achieved applying voltage to the LC cells. Since our aim is to improve the imaging performance of the SLM,

the phase modulation is crucial. The phase-mostly operation accessible in twisted cells will be excluded from the discussion and only the phase-only modulation implemented with linearly polarized light will be considered. In this case, the action of the SLM can be defined by the function $t \propto \exp[i\Phi(\mathbf{r}_\perp, \lambda_0)]$, where \mathbf{r}_\perp determines the position on an active surface of the SLM and λ_0 is the chosen design wavelength. The phase map addressed on the SLM is controlled by the spatial variations of the refractive index n achieved by the applied voltage. The refractive index is adjusted in order to achieve the desired phase profile for a fixed thickness of the LC layer d and the design wavelength λ_0 , $\Phi(\mathbf{r}_\perp, \lambda_0) = 2\pi dn(\mathbf{r}_\perp)/\lambda_0$. If the SLM is illuminated by the monochromatic light with the wavelength λ_0 , a perfect phase modulation is performed. When using the broadband light with the central wavelength λ_0 and the spectral bandwidth $\delta\lambda$, dispersion effects must be taken into account. The refractive index is no longer constant at the given position, but becomes dependent on the wavelength λ due to the normal dispersion of the LC material. As will be shown later, the material LC dispersion is not significant in comparison with the diffractive dispersion. The dispersion associated with the diffraction effects becomes apparent when the spectral component with the wavelength λ is phase modulated and monitored during free-space propagation. Its complex amplitude at the position \mathbf{r}' can be formally written as $\psi(\mathbf{r}', \lambda) \propto \text{FrT}_\lambda \{ \exp[i\Phi(\mathbf{r}_\perp, \lambda_0)] \}$, where FrT_λ denotes the Fresnel transform, whose kernel depends on the wavelength of the modulated wave. As a consequence, the spatial distribution of the complex amplitude $\psi(\mathbf{r}', \lambda)$ is different for the separate spectral components. This effect is known as the diffractive dispersion. In order to operate the SLM in an optimal mode when using the broadband light, a corrective transformation $T(\mathbf{r}, \lambda)$ must be added to the desired phase modulation. Due to this action, the dispersion is eliminated, $\psi(\mathbf{r}', \lambda) = \psi(\mathbf{r}', \lambda_0)$, so that $\psi(\mathbf{r}', \lambda_0) \propto \text{FrT}_\lambda \{ T(\mathbf{r}, \lambda) \exp[i\Phi(\mathbf{r}_\perp, \lambda_0)] \}$. The difficulty of implementation of the proper dispersion compensation is given by the desired phase modulation. The diffractive dispersion was successfully corrected for a linear phase modulation required for angular deflection of light beams. In the spiral phase contrast microscopy [11], the dispersion correction was assured by a double phase modulation of light at the SLM, whose display was divided into the working and correcting area. In another experimental configuration of spiral microscopy [12], the dispersion caused by the linear phase mask addressed on the SLM was compensated by the additional grating inserted into the system.

In this paper, the correction of the diffractive dispersion of the SLM is for the first time demonstrated in applications, where the SLM is addressed by a lens-like pattern and illuminated by a broadband light. In this case, the phase function Φ is quadratic in $|\mathbf{r}_\perp|$. In previous papers, the spectral change of the focal length of the lens function was compensated for three selected wavelengths by an exchange of the phase patterns on the SLM performed synchronously with the switching of a tunable spectral filter [13]. The correction proposed in this paper is based on a mutual elimination of the material dispersion of the corrector and the diffractive dispersion of the SLM. Even in a cooperation with the corrector, the SLM works as an independent device. Its initial operation is maintained for the central wavelength, and only other spectral components are influenced. To achieve such a regime, the corrector is designed in such a way that its optical power is zero for the central wavelength. The quadratic phase modulation with the dispersion correction is useful for imaging applications, optical manipulations or digital holography, but an exceptional impact can be expected in the FINCH experiments [9]. This promising method allows the holographic reconstruction of objects recorded in spatially incoherent light and its application potential has been demonstrated by a number of experiments involving a violation of the Lagrange invariant [14, 15], an exceeding of the diffraction resolution limit [16] or a spiral edge contrast enhancement of 3D objects [17]. In the current FINCH experiments, the light with an extremely narrow spectrum of several nanometers must be used, which deteriorates the signal to noise ratio. Compensation of the diffractive dispersion moves experiments closer to

the physical limits found in [18], that allow the white light high-resolution correlation imaging.

In the paper, the characteristics of the material and diffractive dispersion are briefly summarized and basic design concepts of the dispersion compensation outlined. Subsequently, computer simulations of the chromatic focal shift and the imaging performance of the implemented achromatic system are presented and compared with the results of measurements.

2. Characteristics of material and diffractive dispersion

2.1. Material dispersion of a singlet lens

The material dispersion is characterized by the Abbe number, which can be easily introduced for a singlet lens. If the lens optical power is evaluated for light with the wavelength λ_0 , it can be written as $K(\lambda_0) = [n(\lambda_0) - 1]C$, where $n(\lambda_0)$ is the refractive index of the lens glass and C is a shape factor given by the radius of curvature of the surfaces, $C = 1/R_1 - 1/R_2$. Near λ_0 , the optical power changes with the wavelength as

$$\frac{dK}{d\lambda}\bigg|_{\lambda_0} = \frac{K(\lambda_0)}{[n(\lambda_0) - 1]} \frac{dn}{d\lambda}\bigg|_{\lambda_0}. \quad (1)$$

When light with the spectral range $\lambda \in < \lambda_1, \lambda_2 >$ is used, where $\lambda_{1,2} = \lambda_0 \mp \delta\lambda/2$, the change of the power in this interval, $\delta K(\lambda_1, \lambda_2) = K(\lambda_1) - K(\lambda_2)$, can be written as [19]

$$\delta K(\lambda_1, \lambda_2) = \frac{K(\lambda_0)}{V_M}, \quad (2)$$

where V_M is the Abbe number that defines the material dispersion of the lens as

$$V_M = \frac{n(\lambda_0) - 1}{n(\lambda_1) - n(\lambda_2)}. \quad (3)$$

For the normal material dispersion, the Abbe number is positive and its value depends on the type of glass and the evaluated spectral interval. For the visible spectral region represented by the Fraunhofer lines D, F and C, the Abbe number with values from 20 to 65 is available for common optical glasses.

2.2. Diffractive dispersion of the SLM

In this paper, the dispersion compensation is examined in applications, where the SLM works as a diffractive lens with the desired focal length $f_0 \equiv f(\lambda_0)$. By applying voltage to the individual LC cells, such a change of the refractive index across the SLM surface is set to get the local changes of the optical path given as $dn(\mathbf{r}_\perp) \propto \text{mod}[\lambda_0, |\mathbf{r}_\perp|^2/(2f_0)]$, where d is the thickness of the LC cell and λ_0 denotes the design wavelength. For light with the wavelength λ_0 diffracted in the first order, changes of the optical path correspond to the SLM function with a quadratic phase

$$t = \exp[i\Phi(\mathbf{r}_\perp)], \quad \text{where} \quad \Phi(\mathbf{r}_\perp) = \frac{\pi}{\lambda_0} \frac{|\mathbf{r}_\perp|^2}{f_0}. \quad (4)$$

The diffractive dispersion can be assessed assuming that the plane wave with the spectral bandwidth $\delta\lambda$ is phase modulated by the SLM function t . To exclude an influence of the material LC dispersion at this moment, we assume that the refractive index does not vary with the wavelength. Using the Fourier decomposition, the phase modulation and subsequent free-space

propagation of spectral components can be described by the Fresnel transform as $\psi \propto \text{FrT}_\lambda \{t\}$. After performing the Fresnel transform, we get

$$\psi(\mathbf{r}', \lambda) \propto \exp\left(i\frac{\pi|\mathbf{r}'_\perp|^2}{\lambda z'}\right) \text{FT} \left\{ \exp\left[i\pi|\mathbf{r}_\perp|^2 \left(\frac{1}{\lambda_0 f_0} - \frac{1}{\lambda z'}\right)\right] \right\}, \quad (5)$$

where FT denotes the 2D Fourier transform performed with the spatial frequencies $\mathbf{r}'_\perp/(\lambda z')$, and the used position vectors are defined as $\mathbf{r}_\perp = (x, y)$ and $\mathbf{r}' = (\mathbf{r}'_\perp, z')$. At the propagation distance given as

$$z' \equiv f(\lambda) = \frac{\lambda_0}{\lambda} f_0, \quad (6)$$

the quadratic term in (5) vanishes and the Fourier transform results in the Dirac delta function, $\delta(\mathbf{r}'_\perp)$. As is evident, each spectral component having the wavelength λ is focused to the point lying at the distance (6) from the active surface of the SLM. These distances represent the focal lengths of the SLM lens for individual wavelengths of the used light. As in the case of the material dispersion, a change of the optical power in the interval of wavelengths $< \lambda_1, \lambda_2 >$ can be evaluated. By using (6) and with $K(\lambda_0) = 1/f_0$, we obtain

$$\delta K(\lambda_1, \lambda_2) = \frac{K(\lambda_0)}{V_D}, \quad (7)$$

where V_D represents the Abbe number for the diffractive dispersion [20] given as

$$V_D = \frac{\lambda_0}{\lambda_1 - \lambda_2}. \quad (8)$$

If the Abbe number is evaluated for D, F and C lines, the extremely strong negative dispersion of the SLM is revealed, $V_D = -3.48$.

Combination of material and diffractive dispersion of the SLM

In real conditions, the material dispersion also occurs and its impact must be assessed in a comparison with the diffractive dispersion. In this case, the refractive index is not determined only by the applied voltage, but its value at the local position depends also on the wavelength of incident light. The phase function of the SLM (4) then must be modified to the form

$$t(\lambda) = \exp[i\Phi(\mathbf{r}_\perp, \lambda)], \quad \text{where} \quad \Phi(\mathbf{r}_\perp, \lambda) = \frac{\pi}{\lambda_0} \frac{n(\lambda)}{n(\lambda_0)} \frac{|\mathbf{r}_\perp|^2}{f_0}, \quad (9)$$

where $n(\lambda) \equiv n(\mathbf{r}_\perp, \lambda)$ and $n(\lambda_0) \equiv n(\mathbf{r}_\perp, \lambda_0)$. If the SLM is illuminated by a broadband light and propagation of the spectral components is described by the Fresnel transform, $\psi \propto \text{FrT}_\lambda \{t(\lambda)\}$, the reduction of a quadratic phase term resulting in the Dirac delta function gives the focal length of the SLM as

$$f(\lambda) = \frac{n(\lambda_0)}{n(\lambda)} \frac{\lambda_0}{\lambda} f_0. \quad (10)$$

The change of the optical power for the wavelengths λ_1 and λ_2 can then be written by the corresponding refractive indices $n(\lambda_1)$ and $n(\lambda_2)$ as

$$\delta K(\lambda_1, \lambda_2) = \frac{K(\lambda_0)}{V_{MD}}, \quad (11)$$

where V_{MD} is the Abbe number of the SLM including both the material and diffractive dispersion. It can be written in the same form as in the case of the diffractive dispersion (7), but the modified wavelengths must be used

$$V_{MD} = \frac{\Lambda_0}{\Lambda_1 - \Lambda_2}, \quad (12)$$

where $\Lambda_j = n(\lambda_j)\lambda_j$, $j = 0, 1, 2$. The refractive indices of the LC materials used in display applications were measured in dependence on the temperature for the wavelengths related to D, F and C lines [21]. The Abbe number calculated for ordinary or extraordinary refractive index corresponds to values $V_M \approx 40$ for LC materials with a small birefringence while the materials with a high birefringence show the greater dispersion with $V_M \approx 17$. If the Abbe number including both material and diffractive dispersion (12) is calculated for the lines D, F and C using the refractive indices of the LC material with $V_M = 40$ and 17, we obtain $V_{MD} = -3.57$ and -3.77 , respectively. The inclusion of the LC material dispersion only very weakly reduces the diffractive dispersion for which the Abbe number $V_D = -3.48$ was previously established. Two conclusions arise from the analysis: - the diffractive dispersion of the SLM cannot be significantly reduced with the available LC materials and an external corrector must be used for its elimination, - the material LC dispersion can be disregarded and an approximation $V_{MD} \approx V_D$ adopted in the corrector design.

3. Design concepts for compensation of diffractive dispersion of the SLM

The Abbe number characterizing the material and diffractive dispersion takes positive and negative values, respectively. This fact is well known and has been successfully utilized in hybrid achromatic doublets [20, 22–24], where the diffractive surface has been used to compensate the chromatic aberration of the refractive surface. In this paper, the reverse problem is solved. The diffractive surface is not used as a compensating element but on the contrary an extremely strong diffractive dispersion of the SLM lens is compensated using the refractive dispersion. In the proposed design, the SLM is retained as an independent device cooperating with an external refractive corrector. When using the corrector, the SLM operation remains unaffected for the central wavelength and the diffractive dispersion is eliminated for the other spectral components. The basic idea of the dispersion correction is shown in Fig. 1. The refractive corrector illustrated in Fig. 1(a) eliminates the diffractive dispersion and its action has no effect on the spectral component of light corresponding to the design wavelength of the SLM. Light with the central wavelength λ_0 and the spectral bandwidth $\delta\lambda$ is collimated and directed towards the two-component corrector. While the central wavelength remains unchanged behind the corrector, the spectral components of shorter and longer wavelengths become convergent and divergent waves, respectively. By this way, the diffractive dispersion of the SLM shown in Fig. 1(b) can be compensated. When the chromatic aberration of the corrector is properly implemented, an achromatic operation of the SLM illustrated in Fig. 1(c) can be achieved.

3.1. Achromatic SLM correction by a two-lens afocal system

Design of the corrector is based on the achromatic elimination of the diffractive dispersion of the SLM for the boundary wavelengths of the used spectrum λ_1 and λ_2 . Assuming that the corrector is composed of two lenses, the spectral change of the optical power of the SLM, $\delta K_D(\lambda_1, \lambda_2)$, must be compensated by the changes of the optical power of the lenses $\delta K_1(\lambda_1, \lambda_2)$ and $\delta K_2(\lambda_1, \lambda_2)$, so that $\sum_j \delta K_j(\lambda_1, \lambda_2) = 0$, $j = 1, 2, D$. In order to maintain operation of the SLM unaffected for the central wavelength, the total power of the corrector must be zero. It is achieved, if it consists of a positive and negative lens, whose focal lengths for the

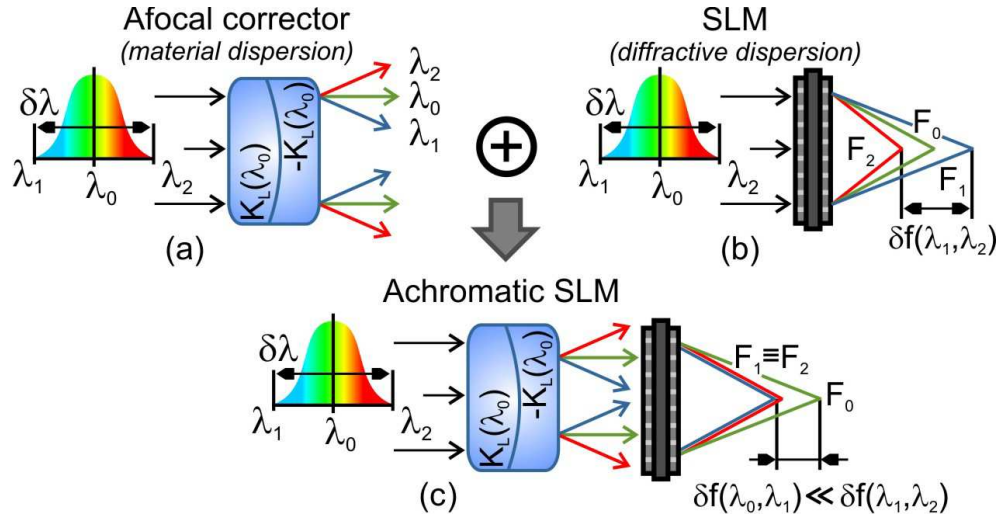


Fig. 1. Concept of the dispersion compensation of the SLM: (a) material dispersion of the afocal refractive corrector, (b) diffractive dispersion of the SLM, (c) achromatic correction of the SLM.

wavelength λ_0 are $f_L(\lambda_0)$ and $-f_L(\lambda_0)$, respectively. Using (2) and (7), the condition ensuring the achromatic correction of the SLM by means of the afocal corrector can be written as

$$\frac{1}{V_1} - \frac{1}{V_2} + \frac{1}{\kappa V_D} = 0, \quad (13)$$

where V_1 , V_2 and V_D denote the refractive and diffractive Abbe number of the corrector lenses and the SLM, respectively. The coefficient κ is an important design parameter defined as

$$\kappa = \frac{f_D(\lambda_0)}{f_L(\lambda_0)}, \quad (14)$$

where $f_D(\lambda_0)$ is the focal length of a diffractive lens displayed on the SLM. Graphical illustration of the condition (13) providing the achromatic correction is in Fig. 2. For low values

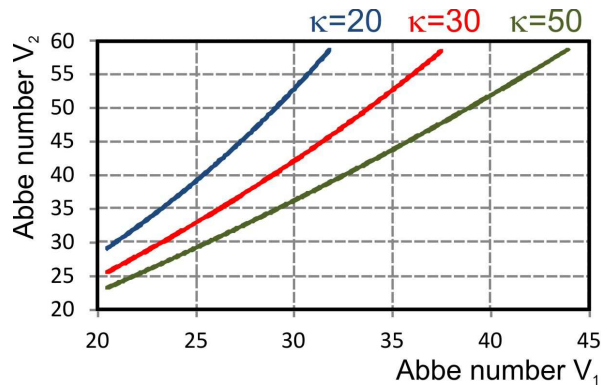


Fig. 2. Combinations of the Abbe numbers of the corrector lenses providing an achromatic correction of the SLM for different values of the design parameter κ .

of the condition (13) providing the achromatic correction is in Fig. 2. For low values

of κ , the choice of the Abbe number V_1 is strongly reduced and only glasses that have small V_1 may be used. For higher values of V_1 , the achromatic correction requires extremely large V_2 , which is not possible with conventional glasses. When κ is increased, the glasses with the Abbe number lying in a wide range of values can be combined. In the design of the corrector, the coefficient $\kappa \approx (20 - 50)$ is applicable. For $\kappa < 20$, the choice of glasses is problematic, and for $\kappa > 50$, a correction of monochromatic aberrations becomes very difficult.

3.2. Secondary spectrum and restrictions for apochromatic correction of the SLM

As was demonstrated, the achromatic correction of the diffractive SLM lens with the focal length $f_D(\lambda_0)$ can be achieved for light with the wavelengths λ_1 and λ_2 . This is possible if the Abbe numbers of the corrector lenses V_1 and V_2 are appropriately adapted to their focal lengths $f_L(\lambda_0)$ and $-f_L(\lambda_0)$. For application of the achromatic system, estimation of the paraxial secondary spectrum is also important. The secondary spectrum from λ_0 to λ_1 is defined as $\delta f(\lambda_0, \lambda_1) = f(\lambda_0) - f(\lambda_1)$, where $f(\lambda_0)$ and $f(\lambda_1)$ is the focal length of the achromatic system composed of the corrector and the SLM for the related wavelengths. When the change of the optical power of the achromatic system is obtained as a sum of the changes of the optical powers of the individual components, $\delta K(\lambda_0, \lambda_1) = \sum_j \delta K_j(\lambda_0, \lambda_1)$, $j = 1, 2, D$, it can be related to the focal length of the system as

$$\delta K(\lambda_0, \lambda_1) = \frac{1}{f(\lambda_0)} - \frac{1}{f(\lambda_1)} \approx -\frac{\delta f(\lambda_0, \lambda_1)}{f^2(\lambda_0)}. \quad (15)$$

The chromatic focal shift then can be obtained as

$$\delta f(\lambda_0, \lambda_1) = \frac{f^2(\lambda_0)}{f_L(\lambda_0)} \left[\frac{P_1}{V_1} - \frac{P_2}{V_2} + \frac{P_D}{\kappa V_D} \right], \quad (16)$$

where $f_L(\lambda_0)$ and $f_D(\lambda_0)$ are the focal lengths of the first corrector lens and the SLM lens for λ_0 , and κ is given by (14). P_1 , P_2 and P_D denote the partial dispersion ratio for the corrector lenses and the SLM, respectively,

$$P_j = \frac{n_j(\lambda_1) - n_j(\lambda_0)}{n_j(\lambda_1) - n_j(\lambda_2)}, \quad j = 1, 2, \quad (17)$$

$$P_D = \frac{\lambda_1 - \lambda_0}{\lambda_1 - \lambda_2}, \quad (18)$$

where n_1 and n_2 are the refractive indices of the corrector lenses for the specified wavelengths. When the chromatic focal shift is applied together with the condition of the achromatic correction (13), the paraxial secondary spectrum is obtained as

$$\delta f(\lambda_0, \lambda_1) = \frac{f^2(\lambda_0)}{f_L(\lambda_0)} \left[\frac{P_1 - P_D}{V_1} - \frac{P_2 - P_D}{V_2} \right]. \quad (19)$$

To achieve the apochromatic correction of the SLM with $\delta f(\lambda_0, \lambda_1) = 0$, the partial dispersion ratio of the corrector lenses and the SLM must be adapted to each other, $P_1 = P_2 = P_D$. Another condition of the apochromatic correction requires $V_1/V_2 = (P_1 - P_D)/(P_2 - P_D)$. For the visible spectral region, optical glasses having the desired partial dispersion ratio are not available, so that a nonzero secondary spectrum must be accepted. In the infrared spectral region, the situation is much more favorable. For the central wavelength about $1.4\mu\text{m}$, the partial dispersion ratios of the available glasses and the SLM are very close, so the apochromatic correction of the SLM operating with the wavelength $1.55\mu\text{m}$ is possible.

4. Optimized design of the corrector for achromatic operation of the SLM

A possibility of implementing the achromatic correction of the SLM by a two-component refractive system was demonstrated by the condition (13) that determined a connection between the Abbe number of the corrector glasses and the geometrical factor κ . The two-lens system was used to simplify demonstration of the achromatic operation of the SLM, but in the optimized design, the three-lens system was applied. Distribution of the optical power into three lenses resulted to a reduction of the coefficient κ , which allowed an acceptable correction of the monochromatic aberrations. In the first stage of the design, a selection of glasses and factors κ was performed using the achromatic condition obtained by a straightforward generalization of (13) for the three-lens system and consequently the final optimization of parameters was carried out in Oslo Premium software.

When addressing a lens-like pattern on the SLM, the focal length cannot be arbitrarily chosen but the smallest possible value is determined by parameters of the device. A quadratic phase of the lens Φ is reduced to the interval $< 0, 2\pi >$, so that a quasi-periodic pattern with the highest spatial frequency ν_m at the edge of the SLM is obtained,

$$\nu_m = \frac{1}{2\pi} \frac{\partial \Phi(\mathbf{r}_\perp)}{\partial |\mathbf{r}_\perp|} \Big|_{|\mathbf{r}_\perp|=R}, \quad (20)$$

where $2R$ is the size of the SLM display. If the Nyquist-Shannon sampling theorem is respected, the shortest focal length that can be addressed on the SLM is given as

$$f \geq \frac{2\Delta r R}{\lambda}, \quad (21)$$

where Δr denotes the pixel size of the used SLM. For example, for $2R=15\text{mm}$, $\Delta r=15\mu\text{m}$ and $\lambda=500\text{nm}$, the shortest addressable focal length is $f \approx 450\text{mm}$. In the design of the corrector, the focal length of the SLM lens $f_D(\lambda_0)=500\text{mm}$ was taken for the design wavelength corresponding to the D line, $\lambda_0=589\text{nm}$. The achromatic correction was required for F and C lines, $\lambda_1=486\text{nm}$ and $\lambda_2=656\text{nm}$. If the uncompensated SLM was used, the diffractive dispersion resulted in the chromatic focal shift $\delta f_D(\lambda_1, \lambda_2) = -f_D(\lambda_0)/V_D$. For D, F and C lines giving the Abbe number $\nu_D = -3.5$ and $f_D=500\text{mm}$, an extremely large focal shift $\delta f_D \approx 143\text{mm}$ was obtained. With the designed three-lens system, the achromatic correction for the F and C lines was reached and the secondary spectrum was reduced to an acceptable level.

When using white light, the diffraction efficiency of the SLM lens is also affected. An ideal diffractive lens with the quadratic phase reduced to the interval $< 0, 2\pi >$, $\Phi = \text{mod}[2\pi, \pi|\mathbf{r}_\perp|^2/(\lambda_0 f_0)]$, focuses all the light into the first diffraction order related to the focal length f_0 . This happens only if the monochromatic light with the design wavelength λ_0 is used [25]. If the diffractive lens is illuminated by light of a different wavelength λ , unwanted diffraction orders are created and multiple foci appear. The diffraction efficiency in the m -th order depends on the wavelength detuning and can be written as

$$\eta_m(\lambda) = \text{sinc}^2 \left[\pi \left(\frac{\lambda_0}{\lambda} - m \right) \right], \quad (22)$$

where $\text{sinc}(x) \equiv \sin x/x$. For light with the central wavelength λ_0 and the spectral range $\lambda \in < \lambda_1, \lambda_2 >$, the polychromatic integrated efficiency [26, 27] can be defined by

$$\bar{\eta}_m = \frac{1}{\lambda_2 - \lambda_1} \int_{\lambda_1}^{\lambda_2} \eta_m(\lambda) d\lambda. \quad (23)$$

For the spectral interval specified by the lines D, F and C, the integrated efficiency $\bar{\eta}_1 \approx 0,97$ is obtained in the first diffraction order. This means that 97% of the energy of input polychromatic light is concentrated in the first-order focus, while the remaining energy is divided

into the higher-order foci. Light in the higher diffraction orders creates a bright background deteriorating the image contrast. In [26], an influence of the integrated diffraction efficiency on the modulation transfer function was examined showing that only lower spatial frequencies are slightly affected by the background-order light. White light diffracted into the first order is not still focused into a single point specified by the focal length f_0 , because the focal length becomes a function of the wavelength, $f = f_0 \lambda_0 / \lambda$. This diffractive dispersion causes deterioration of the image quality, which is much stronger than the reduction of the contrast due to the polychromatic diffraction efficiency. When designing the refractive corrector, the main attention was focused on the achromatic correction of the diffractive dispersion of the SLM without considering changes in the diffraction efficiency.

An apparent increasing of the optical performance of the corrected SLM was demonstrated by the measurement of the system implemented in a cooperation with Meopta Přerov company.

5. Experimental testing of the achromatic SLM

5.1. Measurement of the chromatic focal shift

To verify the spectral properties of the examined systems, the chromatic focal shift of the uncorrected SLM and the secondary spectrum of the SLM supplemented by the afocal corrector were measured by means of the Shack-Hartmann (S-H) wavefront sensor. The used experimental setup is shown in Fig. 3. The laser beams with the wavelengths 532nm, 472nm and 632.8nm approaching the Fraunhofer lines D, F and C were coupled into the single-mode fibers and sequentially collimated by the achromatic lens and directed toward the SLM. In all measurements, the SLM was addressed by a fixed lens-like pattern providing the focal length $f_D=500\text{mm}$ for the design wavelength 532nm. The position of the focal point behind the SLM was determined from the wavefront measurement carried out by the S-H sensor. The wavefront diagnostics was implemented in a reference mode to avoid imperfections of the used optical elements, adjusting inaccuracies and an influence of the secondary spectrum of the achromatic lens. The initial reference measurement was carried out without the corrector using only uninitiated SLM operating as a plane mirror. After that calibration, the lens phase was displayed on the SLM and the focused wave captured by the S-H sensor. The same measurement was repeated with the corrector placed in front of the SLM. The detected wavefronts were processed relative to the reference wavefront and the focal points determined. From the positions of the focal points assigned for three wavelengths, the chromatic focal shift was evaluated. In Fig. 4, the measured values are compared with the results of calculations. The chromatic focal shift of the SLM caused by the extremely strong diffractive dispersion is illustrated in blue. The secondary spectrum of the SLM cooperating with the afocal refractive system is shown in red. In this case, the operation of the SLM was achromatic and its secondary spectrum was reduced to an acceptable value of 25 mm.

5.2. Evaluation of the imaging performance

To evaluate the imaging performance of the uncorrected and achromatic SLM, the modulation transfer function (MTF) was calculated for broadband light and compared with the contrast of the USAF resolution target measured for the selected spatial frequencies. The used setup is shown in Fig. 5. Light from a halogen lamp was transmitted through the hot mirror and the green filter (532nm, FWHM 80nm) and coupled into a liquid light guide. Light emerging from the fiber guide was used for illumination of the USAF resolution target and after passing through the beam splitter it was collimated by an achromatic lens with the focal length 100mm. When testing the uncorrected SLM (Hamamatsu X10468, 800x600 pixels), the collimated beam was directed toward the SLM addressed by the phase function of the lens with the focal length $f_D=500\text{mm}$ for $\lambda_0=532\text{nm}$. The polarizer and iris diaphragm were inserted in front of the SLM

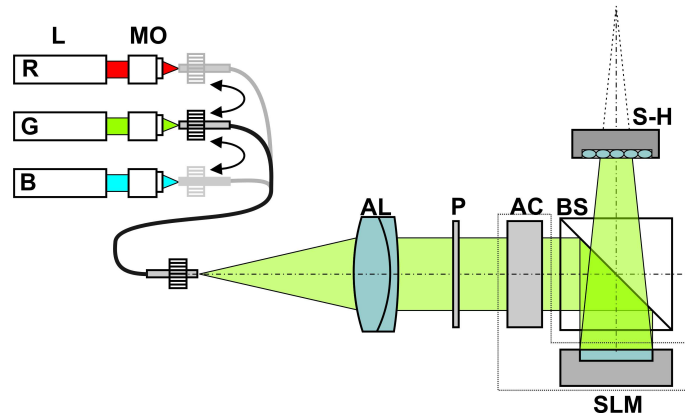


Fig. 3. Experimental setup for measurement of the chromatic focal shift of the SLM and the secondary spectrum of the corrected SLM by means of the S-H sensor: L ... laser, MO ... microscope objective, AL ... achromatic lens, AC ... three-lens afocal corrector, BS ... beam splitter, P ... polarizer.

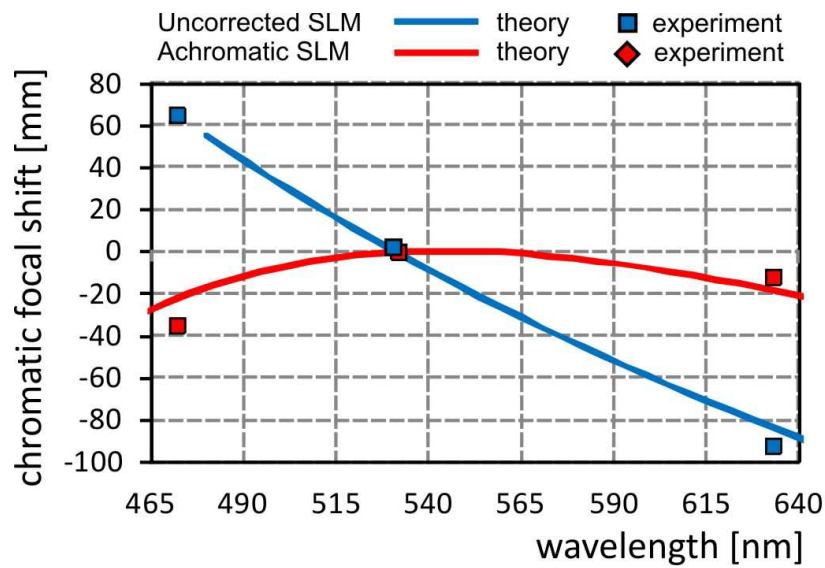


Fig. 4. The measured and calculated chromatic focal shift for the uncorrected SLM with extremely strong diffractive dispersion (blue) and the achromatic correction of the SLM carried out by a three-lens afocal system (red).

to reach the phase only modulation and to control the size of the numerical aperture. Image of the USAF target was detected at the focal plane of the SLM lens by means of the CMOS camera (uEye ui-641). The detected image was processed and contrast of the groups of the target with 10, 20 and 40 cycles/mm evaluated.

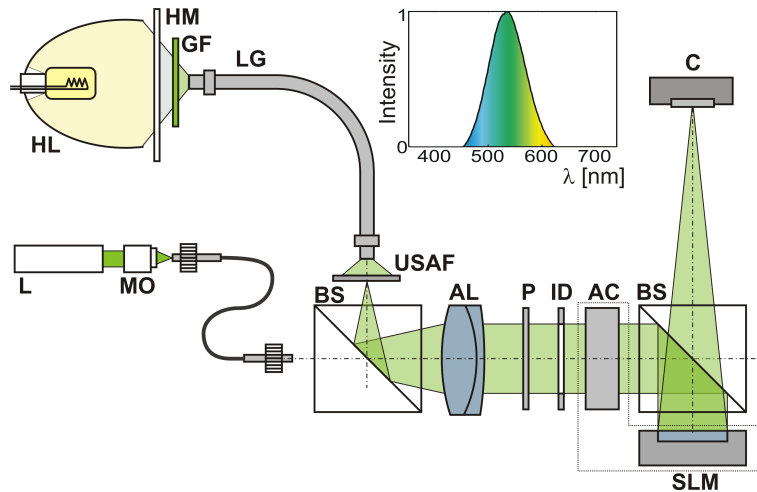


Fig. 5. Testing of the imaging performance of the uncorrected and achromatic SLM by means of the USAF resolution target: HL ... halogen lamp, HM ... hot mirror, GF ... green filter, ... LG light guide, L ... laser, MO ... microscope objective, BS ... beam splitter, AL ... achromatic lens, AC ... afocal corrector, P ... polarizer, ID ... iris diaphragm, C ... CMOS camera.

In the subsequent measurement, the refractive afocal corrector ensuring an achromatic operation of the SLM was used. Before the measurement, a laser beam with the wavelength 532nm coupled into the single-mode fiber and collimated by the microscope objective was used to achieve a precise alignment of the system. The image contrast of the selected groups of the USAF target was evaluated for two different diameters of the iris diaphragm 4mm and 12mm, corresponding to the numerical aperture of the collimating lens $NA=0.02$ and 0.06 , respectively. The measured data are shown in Fig. 6 together with the MTF calculated in Oslo Premium software. In the calculations, the theoretical design parameters of the corrector were used, and the SLM lens was defined as a diffractive surface (symmetric CGH) of the second kinoform construction order. Weights of the wavelengths used in the calculation of the polychromatic MTF were adapted to the transmission of the green filter. Results in Fig. 6(a) correspond to the small aperture, $NA=0.02$, for which the achromatic SLM reached the diffraction imaging limit. As is evident, a strong diffractive dispersion of the uncorrected SLM apparently degraded image even when a small aperture was used. The surprising fact that the measured data slightly exceeded the theoretical values can be explained by differences in the evaluation of the image contrast. While the demonstrated MTF calculations were performed with the cosine gratings, the image of the rectangular gratings of the resolution target was processed in the measurement. A slight improvement of the image contrast is well known, in this case. In Fig. 6(b), the results of the contrast measurement and the MTF calculations are illustrated for the numerical aperture of the collimating lens $NA=0.06$. The achromatic correction significantly increased the imaging performance of the SLM compared to the uncorrected state. According to both the theoretical and experimental results, the image contrast was increased nearly four times for higher spatial frequencies. Even with the achromatic correction, the image performance was still reduced due

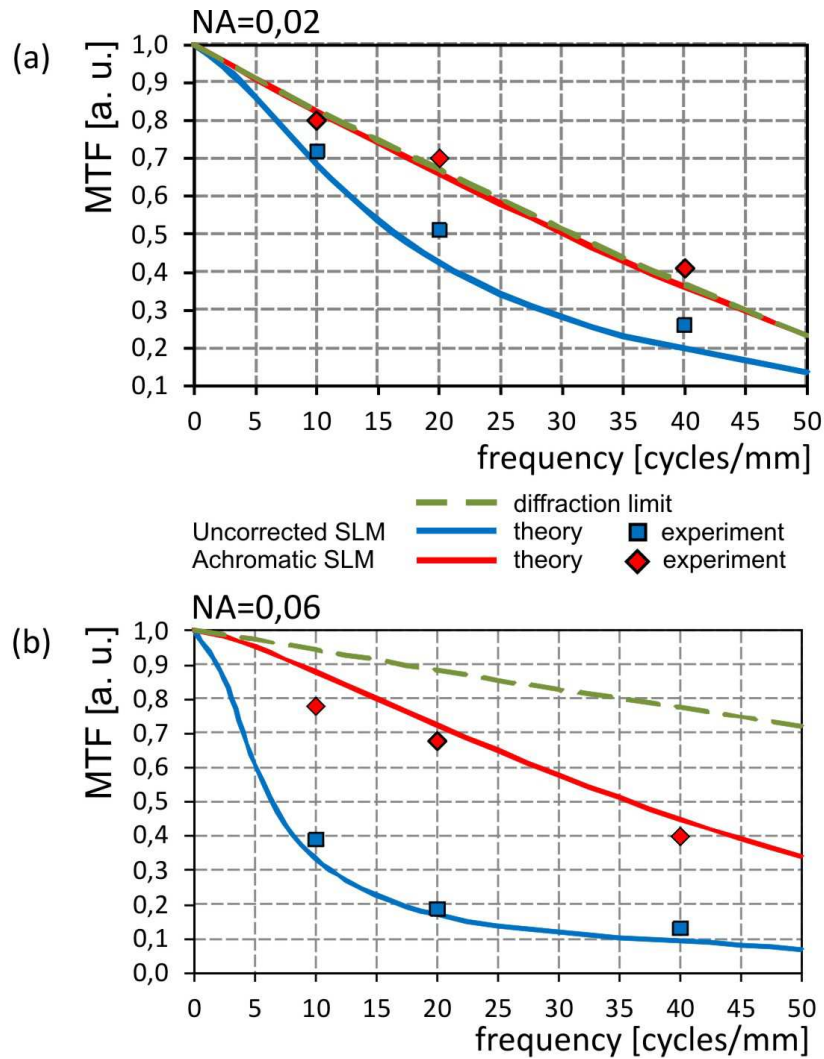


Fig. 6. Measured contrast (10, 20 and 40 cycles/mm) and the calculated modulation transfer function for the imaging implemented by the uncorrected and achromatic SLM: (a) NA=0.02, (b) NA=0.06.

to the secondary spectrum. To reach the diffraction limit with the high numerical apertures, the apochromatic correction is required. Image frames of the USAF target acquired by uncorrected and achromatic SLM are compared in Fig. 7.

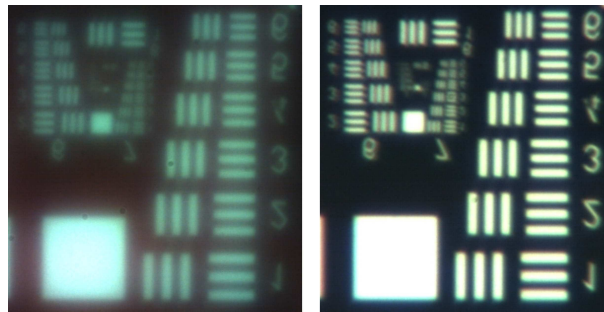


Fig. 7. Snapshots of the USAF resolution target taken in the broadband light (532 nm, FWHM 80 nm): uncorrected SLM (left), achromatic SLM (right).

6. Conclusions

In the paper, the SLM working as an imaging element in the broadband light was investigated and the elimination of degradation effects caused by the strong diffractive dispersion proposed. As the main result, the refractive corrector was designed and implemented, that enabled the achromatic operation of the SLM in the entire visible spectral region. Specifically, the following results were obtained:

- The Abbe number involving material and diffractive dispersion was derived and used for analysis of the SLM action in white-light illumination.
- Optical system having zero optical power for the central wavelength and providing an achromatic correction of the diffractive dispersion of the SLM was designed, manufactured and successfully tested in imaging experiments.
- Apochromatic correction of the SLM was discussed and a possibility to reach it in the infrared spectral region outlined.

Although the correction of the diffractive dispersion can be useful for variety of applications in imaging and metrology, its main significance can be expected in the FINCH experiments, where the SLM operates as a beam splitter ensuring holographic recording of 3D objects in spatially incoherent light [9]. The achromatic compensation of the diffractive dispersion and successfully elaborated apochromatic correction of the SLM in the visible region represent an important progress on the pathway towards the white light high-resolution correlation microscopy outlined in [18].

Acknowledgments

This work was supported by the IGA project of the Palacký University PrF 2014-14, the project CEITEC - “Central European Institute of Technology” No. CZ.1.05/1.1.00/02.0068 from European Regional Development Fund and the project POST-UP II, No. CZ.1.07/2.3.00/30.0041 from European Social Fund in the Czech Republic. The refractive corrector was realized in a cooperation with Meopta Přerov company in the framework of the project No. TE01020229 of the Technology Agency of the Czech Republic.